Flow Measurement and Instrumentation 69 (2019) 101582

Contents lists available at ScienceDirect

Flow Measurement and Instrumentation

journal homepage: www.elsevier.com/locate/flowmeasinst

Combining measurements with models for superior information in hydropower plants

Liubomyr Vytvytskyi, Bernt Lie*

University of South-Eastern Norway, Porsgrunn, Norway

ARTICLE INFO

Keywords:
State estimation
Nonlinear Kalman filters
Hydropower
Modelling
OpenModelica

ABSTRACT

Water flow and pressure measurements play essential roles in the operation of hydropower plants. For all methods of measuring flow and pressure, there is a level of uncertainty with regards to sensor noise and sensor failure. In addition, measurements in key locations are hard to obtain. A combination of measurements with a mathematical model of a hydropower plant can be used to improve information about and operation of the hydropower system.

This paper describes the possibility of using nonlinear estimators such as Ensemble or Unscented Kalman filters in order to estimate the states of the hydropower system based on water flow and/or pressure measurements. The implementation of the estimators is done in Python using a Python API for operating OpenModelica simulations, where the hydropower system is modeled using an in-house hydropower Modelica library — *OpenHPL*.

1. Introduction

1.1. Background

A transition towards more renewable energy sources is currently taking place in Europe and elsewhere. This situation leads to an increase in the use of flexible hydropower plants to compensate for the profoundly changing production from intermittent energy sources such as wind and solar irradiation. For this reason, the maintenance and optimal management of existing hydropower plants has become a crucial task.

Optimal operation strongly depends on accurate knowledge and monitoring of the ongoing processes via measuring critical quantities of a hydropower system. However, in many cases, some of these quantities of interest cannot be directly measured. Therefore, it is of interest to consider a combination of available measurements with a mathematical model to estimate the needed quantities and improve the quality of information in hydropower plants.

Popular state estimation methods include the Kalman filter (KF) with a wide range of extensions that apply depending on model type, computational effort, etc. Due to nonlinearities in the hydropower model, nonlinear types of KF such as Unscented (UKF) and Ensemble (EnKF) Kalman filters are considered in this study. The classical nonlinear estimator, the Extended Kalman filter (EKF), is widely used, too. However, the EKF assumes the existence of the model state Jacobian, and has relatively poor accuracy due to the linear approximation used in the Kalman gain computation. On the other hand, the UKF and EnKF take more advantage of the nonlinear model in the Kalman gain computation, and theoretically leads to better performances.

1.2. Previous work

Modern state estimation theory appeared in the middle of the 20th century, and since then the data assimilation idea has spread to almost all areas of engineering and science. The basic presentation of a variety of state estimation techniques (standard KF, EKF, UKF, etc.) for a general system is provided in Simon [1]; Julier and Uhlmann [2]. The EnKF is a technique for state and parameter estimation, Evensen [3]. An implementation of the UKF to estimate states of a hydropower plant that balances the uncertainty in pressure measurements, has been demonstrated in Zhou and Glemmestad [4]. The use of the EnKF to predict runoff or groundwater flow for hydrology models that are slightly related to hydropower systems is given in Zou et al. [5] and Shi et al. [6].

State estimation is traditionally used with mechanistic models. However, state estimation can also be used with data driven models, e.g., artificial neural networks (ANN). See, e.g., Murphy [7]; Farrell and Polycarpou [8]. An application of ANN for estimation of hydropower plant water inflow is provided in, e.g., Stokelj and Golob [9]; Sacchi

* Corresponding author.
E-mail addresses: liubomyr.vytvytskyi@usn.no (L. Vytvytskyi), Bernt.Lie@usn.no (B. Lie).

https://doi.org/10.1016/j.flowmeasinst.2019.101582
Received 28 June 2018; Received in revised form 19 November 2018; Accepted 4 March 2019
Available online 12 July 2019

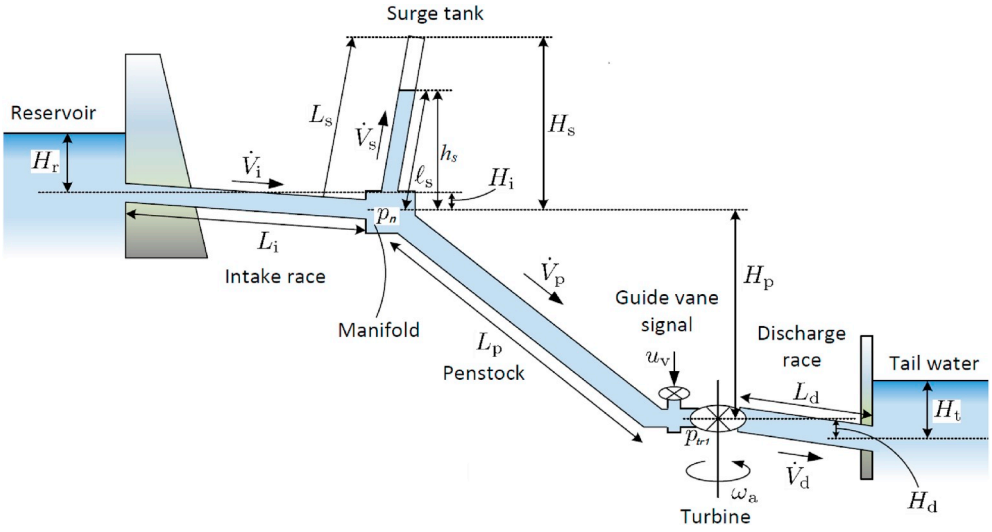

Fig. 1. Overview of the structure of a high head hydropower plant.

et al. [10]. However, data driven models provide a physical interpretation only for the inputs and outputs of the system, while for mechanistic models, internal states and auxiliary variables also have a physical interpretation. This means that with a mechanistic model, it is possible to find internal quantities in the system with some certainty. In data driven models, internal quantities have no physical interpretation unless they are calibrated during an extended and complex experimental phase.

Vytvytskyi and Lie [11,12] discuss work on modelling a waterway for high head hydropower systems together with a generator, the Francis turbine, and a governor using OpenModelica.[1] Unit models have been assembled in our in-house Modelica[2] library *OpenHPL*.

A Python API[3] for OpenModelica already exists which provides possibilities for controlling simulations of the OpenModelica models via Python,[4] Lie et al. [13]. Python in turn, gives much broader possibilities for plotting, analysis, and optimization compared to what is possible in OpenModelica.

1.3. Overview of paper

The main contribution of this paper is an investigation of the possibility of state estimation for a hydropower system using nonlinear Kalman filters. Model implementation is done in OpenModelica using the *OpenHPL* library. The estimators are implemented in Python and use the Python API for OpenModelica.

The paper is structured as follows: Section 2 gives a description of the hydropower system. Details of the Ensemble and Unscented Kalman filters are presented in Section 3. Section 4 gives an overview of the *OpenHPL* library and a presentation of the hydropower model. The results of combining the measurements and models for the hydropower system are described in Sections 5. Finally, discussion and conclusions are given in Section 6.

2. System description

A high head hydropower system is considered for this study, due to its significance in Norway. High head hydropower systems are also more useful for compensating intermittent power than run-of-river systems are, due to their larger buffer capacity from their reservoir.

[1] https://openmodelica.org.
[2] https://www.modelica.org.
[3] https://goo.gl/Qyjqq2.
[4] https://www.python.org.

2.1. System geometry

High head plants typically collect and store water in reservoirs in mountains, with tunnels leading the relatively small flow of water down a considerable height difference to the aggregated turbine and generator. The electricity produced by the generator is then transferred through power lines to consumers. A typical structure for a high head hydropower plant is depicted in Fig. 1, Vytvytskyi and Lie [11].

For simulations in this paper, data from the Sundsbarm hydropower plant in Telemark, Norway is used with data taken from Vytvytskyi and Lie [11]; see Tables 1 and 2.

2.2. Typical measurements

Typically, measurements from the electric part of hydropower plants are readily available in control systems. Also, water levels (main reservoir and tail water, surge tank) are often available.

In this study, a hydropower model of the waterway is considered, assuming constant water level in reservoirs and with additional simplifications introduced in a later section. Water flow and pressure measurements in the waterway units are of interest. In real hydropower plants, only a few of these quantities are measured, e.g., pressure measurements before or after the turbine, water flow rate before the

Table 1
The waterway geometry of the Sundsbarm hydropower plant.

Waterway unit	Height difference, [m]	Length, [m]	Diameter, [m]
Reservoir	48	–	–
Intake race	23	6600	5.8
Penstock	428.5	600	3
Surge tank	120	140	3.4
Discharge	0.5	600	5.8
Tail water	5	–	–

Table 2
The turbine geometry of the Sundsbarm hydropower plant.

Turbine type	Nominal head, [m]	Nominal flow rate, [m^3/s]	Nominal power, [MW]
Francis	460	24.3	104.4

turbine, etc. The turbine flow rate can sometimes also be approximated from the turbine characteristics.

Typically, the accuracy of the pressure measurements in hydropower plants is in the order of 1%. The flow rate measurement errors can be less precise and are in the range of $1-10\%$, depending on how the measurements are done. For simplicity, an accuracy of 1% is assumed for both pressure and flow rate measurements in this work.

We consider three cases of measurements: the turbine flow rate only is measured for one case, the inlet turbine pressure or the manifold node pressure only is available for the second case, and for the third case, both the flow rate and the inlet turbine pressure are measured. It should be noted that for the last case with a combination of two measurements, the "less expensive" solution of two measurements at the same position is chosen, — less expensive in the sense that these will be cheaper to install and maintain.

3. State estimation methods

3.1. Overview

As mentioned above, the hydropower plant model can be highly nonlinear, and use of the widely applied EKF can lead to difficulties in Jacobian computation. Moreover, the EKF rely on a linear approximation to propagate the mean and covariance of the states and this can cause unreliable estimates, Simon [1]. At the same time, the UKF and EnKF are much simpler to use as no Jacobian needs to be computed. Also, they avoid the linearization problem due to use of the unscented transformation and Monte Carlo simulations of the nonlinear model, respectively. These two methods allow approximating the variation of the mean and covariance of random variables that propagate through the nonlinear model.

In Modelica, models are described as differential and algebraic equations (DAEs), with differential and algebraic variables. OpenModelica by default transforms the DAEs into state space form with auxiliary variables: states are typically a subset of the differential variables, while the auxiliary variables are the remaining variables.

Below, a more detailed description of both the UKF and EnKF are given for a nonlinear dynamic system of the form:

$$\begin{aligned} x_k &= f(x_{k-1}, u_{k-1}, w_{k-1}) \\ y_k &= g(x_k, u_k, v_k) \end{aligned} \tag{1}$$

where, $w_k \sim \mathcal{N}(\bar{w}_k, W_k)$, $v_k \sim \mathcal{N}(\bar{v}_k, V_k)$, $x_1 \sim \mathcal{N}(\bar{x}_1, X_1)$.

Here, $x \in \mathbb{R}^{n_x}$ is the state vector with initial state x_1 which is normally distributed. u is a deterministic input signal vector, and $y \in \mathbb{R}^{n_y}$ is a measurement vector. w and v are vectors of random disturbance and measurement noise, respectively. The disturbance and noise are also assumed normally distributed.

In addition, the notations $\hat{x}_{k|k-1}$ and $\hat{x}_{k|k}$ are introduced. Here, $\hat{x}_{k|k-1}$ is the best possible estimate of x_k when information (i.e., sensor signal values) up to and including time index $k-1$ is used, i.e., $\hat{x}_{k|k-1}$ uses measurements $y_1, \ldots, y_{k-2}, y_{k-1}$; $\hat{x}_{k|k-1}$ is denoted the *a priori* estimate. Likewise, $\hat{x}_{k|k}$ is the best possible estimate of x_k when information up to and including time index k is used, i.e., $\hat{x}_{k|k}$ uses the measurements $y_1, \ldots, y_{k-1}, y_k$; $\hat{x}_{k|k}$ is denoted the *a posteriori* estimate. It follows that estimate $\hat{x}_{k|k}$ should be better/more accurate than estimate $\hat{x}_{k|k-1}$.

The covariance estimate of the states is indicated with symbol X_k, thus $X_{k|k-1}$ is the covariance of $\hat{x}_{k|k-1}$, while $X_{k|k}$ is the covariance of $\hat{x}_{k|k}$. It follows that $X_{k|k-1} \geq X_{k|k}$.

3.2. Ensemble Kalman filter

The Ensemble Kalman filter is based on the use of Monte Carlo simulation of the nonlinear system in order to calculate the cross and innovation covariances. Contrary to the EKF, the EnKF does not need Jacobians in the computation.

First, the initial state is assumed to be normally distributed. Hence, *realizations/particles* of the state are randomly generated in the form of $x^i_{1|1} \sim \mathcal{N}(\bar{x}_1, X_1)$, $i \in \{1, \ldots, n_p\}$ where n_p is the number of these realizations/particles. Next, n_p realizations/particles of the state propagates, $x^i_{k|k-1} = f(x^i_{k-1|k-1}, u_{k-1}, w^i_{k-1})$, and measurements $y^i_{k|k-1} = g(x^i_{k-1|k-1}, u_{k-1}, v^i_{k-1})$ are similarly computed. Disturbance w^i_k and measurement noise v^i_k are also randomly generated.

The complete EnKF algorithm is given by the following steps:

1. EnKF initialization, $k = 1$:
   - draw random initial particle values, $i \in \{1, \ldots, n_p\}$:

$$x^i_{1|1} \sim \mathcal{N}(\bar{x}_1, X_1) \tag{2}$$

   - *a posteriori* state estimate:

$$\hat{x}_{1|1} = \frac{1}{n_p} \sum_{i=1}^{n_p} x^i_{1|1} \tag{3}$$

2. Propagation step, $k = 2,3, \ldots$:
   - *a posteriori* covariance estimate:

$$X_{1|1} = \frac{1}{n_p - 1} \sum_{i=1}^{n_p} (x^i_{1|1} - \hat{x}_{1|1})(x^i_{1|1} - \hat{x}_{1|1})^T \tag{4}$$

   - draw random disturbance, $i \in \{1, \ldots, n_p\}$:

$$w^i_k \sim \mathcal{N}(\bar{w}_k, W_k) \tag{5}$$

   - *a priori* state estimate, $i \in \{1, \ldots, n_p\}$:

$$\begin{aligned} x^i_{k|k-1} &= f(x^i_{k-1|k-1}, u_{k-1}, w^i_{k-1}) \\ \hat{x}_{k|k-1} &= \tfrac{1}{n_p} \textstyle\sum_{i=1}^{n_p} x^i_{k|k-1} \end{aligned} \tag{6}$$

   - *a priori* covariance estimate:

$$X_{k|k-1} = \frac{1}{n_p - 1} \sum_{i=1}^{n_p} (x^i_{k|k-1} - \hat{x}_{k|k-1})(x^i_{k|k-1} - \hat{x}_{k|k-1})^T \tag{7}$$

3. Information update, $k = 2,3, \ldots$:
   - draw measurement noise, $i \in \{1, \ldots, n_p\}$:

$$v^i_k \in \mathcal{N}(\bar{v}_k, V_k) \tag{8}$$

   - measurement and innovation, $i \in \{1, \ldots, n_p\}$:

$$\begin{aligned} y^i_{k|k-1} &= g(x^i_{k|k-1}, u_k, v^i_k) \\ \hat{y}_{k|k-1} &= \tfrac{1}{n_p} \textstyle\sum_{i=1}^{n_p} y^i_{k|k-1} \end{aligned} \tag{9}$$

   - cross and innovative covariances:

$$Z_{k|k-1} = \frac{1}{n_p - 1} \sum_{i=1}^{n_p} (x^i_{k|k-1} - \hat{x}_{k|k-1})(y^i_{k|k-1} - \hat{y}_{k|k-1})^T \tag{10}$$

$$\mathscr{E}_{k|k-1} = \frac{1}{n_p - 1} \sum_{i=1}^{n_p} (y^i_{k|k-1} - \hat{y}_{k|k-1})(y^i_{k|k-1} - \hat{y}_{k|k-1})^T \tag{11}$$

   - Kalman gain:

$$K_k = Z_{k|k-1} \mathscr{E}^{-1}_{k|k-1} \tag{12}$$

   - *a posteriori* state estimate, $i \in \{1, \ldots, n_p\}$:

$$x^i_{k|k} = x^i_{k|k-1} + K_k(y_k - y^i_{k|k-1})$$
$$\hat{x}_{k|k} = \frac{1}{n_p}\sum_{i=1}^{n_p} x^i_{k|k} \tag{13}$$

- *a posteriori* covariance estimate:

$$X_{k|k} = \frac{1}{n_p - 1}\sum_{i=1}^{n_p}(x^i_{k|k} - \hat{x}_{k|k})(x^i_{k|k} - \hat{x}_{k|k})^T \tag{14}$$

Based on the similarity to bootstrap statistics, Efron [14]; the number of *realizations/particles* should be equal to, or greater than 50 in order to provide reasonably accurate estimates of mean and covariance. Obviously, it is required that $n_p \geq \min(n_y, n_x)$ to avoid rank loss in the innovation covariance matrix $\mathscr{E}_{k|k-1}$ and the state covariance matrices $X_{k|k-1}$ and $X_{k|k}$.

3.3. Unscented Kalman filter

The main idea of the UKF is closely related to the EnKF in the point that a set of *realizations/particles* are transformed through the nonlinear system, then their results are collected to estimate state mean and covariance. However, in the EnKF the set of n_p *realizations/particles* is randomly generated, whereas in the UKF these points are created based on certain deterministic rules and denoted sigma points, Simon [1].

The sigma points for state vector $x \in \mathbb{R}^{n_x}$ could be defined based on the mean $\bar{x}$ and covariance X of the states by the following algorithm:

$$x^i = \bar{x} + \tilde{x}^i, \quad i \in \{1, ..., 2n_x\} \tag{15}$$

where

$$\tilde{x}^i = (\sqrt{n_x X})^T_i, \quad i \in \{1, ..., n_x\}$$
$$\tilde{x}^{n_x+i} = -(\sqrt{n_x X})^T_i, \quad i \in \{1, ..., n_x\} \tag{16}$$

where $\sqrt{n_x X}$ is the Cholesky root[5] of $n_x X$, i.e., $(\sqrt{n_x X})^T \times \sqrt{n_x X} = n_x X$, while $(\sqrt{n_x X})_i$ is the ith row of $\sqrt{n_x X}$.

In addition to the unscented transformation, other possible transformations exist, e.g., the simplex transformation, the spherical transformation, and others, Simon [1]; Julier and Uhlmann [15]. These additional transformations might be applied when computational savings are of interest, or if there are more statistics of the noise, etc.

Similarly to the EnKF, the UKF algorithm can be described as follows:

1. The UKF initialization, $k = 1$:
   - *a posteriori* state estimate:

$$\hat{x}_{1|1} = \bar{x}_1 \tag{17}$$

2. Propagation step, $k = 2,3, ...$:
   - *a posteriori* covariance estimate:

$$X_{1|1} = X_1 \tag{18}$$

   - find sigma points:

$$x^i_{k-1|k-1} = \hat{x}_{k-1|k-1} + \tilde{x}^i, \ i \in \{1, ..., 2n_x\} \tag{19}$$

   where

$$\tilde{x}^i = (\sqrt{n_x X_{k-1|k-1}})^T_i, \ i \in \{1, ..., n_x\}$$
$$\tilde{x}^{n_x+i} = -(\sqrt{n_x X_{k-1|k-1}})^T_i, \ i \in \{1, ..., n_x\} \tag{20}$$

   - *a priori* state estimate, $i \in \{1, ..., 2n_x\}$:

$$x^i_{k|k-1} = f(x^i_{k-1|k-1}, u_{k-1})$$
$$\hat{x}_{k|k-1} = \frac{1}{2n_x}\sum_{i=1}^{2n_x} x^i_{k|k-1} \tag{21}$$

3. 3. Information update, $k = 2,3, ...$:
   - *a priori* covariance estimate:

$$X_{k|k-1} = \frac{1}{2n_x}\sum_{i=1}^{2n_x}(x^i_{k|k-1} - \hat{x}_{k|k-1})(x^i_{k|k-1} - \hat{x}_{k|k-1})^T + W_k \tag{22}$$

   - measurement and innovation, $i \in \{1, ..., 2n_x\}$:

$$y^i_{k|k-1} = g(x^i_{k|k-1}, u_k)$$
$$\hat{y}_{k|k-1} = \frac{1}{2n_x}\sum_{i=1}^{2n_x} y^i_{k|k-1} \tag{23}$$

   - cross and innovative covariances:

$$Z_{k|k-1} = \frac{1}{2n_x}\sum_{i=1}^{2n_x}(x^i_{k|k-1} - \hat{x}_{k|k-1})(y^i_{k|k-1} - \hat{y}_{k|k-1})^T \tag{24}$$

$$\mathscr{E}_{k|k-1} = \frac{1}{2n_x}\sum_{i=1}^{2n_x}(y^i_{k|k-1} - \hat{y}_{k|k-1})(y^i_{k|k-1} - \hat{y}_{k|k-1})^T + V_k \tag{25}$$

   - Kalman gain:

$$K_k = Z_{k|k-1}\mathscr{E}^{-1}_{k|k-1} \tag{26}$$

   - *a posteriori* state estimate:

$$\hat{x}_{k|k} = \hat{x}_{k|k-1} + K_k(y_k - \hat{y}_{k|k-1}) \tag{27}$$

   - *a posteriori* covariance estimate:

$$X_{k|k} = X_{k|k-1} - K_k\mathscr{E}_{k|k-1}K^T_k \tag{28}$$

It is seen that the number of sigma points equals twice the number of states. This means that for systems with few states, the UKF needs lower computation effort than the EnKF does. It is clearly assumed that $n_y \leq 2n_x$ to avoid rank loss in $\mathscr{E}_{k|k-1}$.

It should be noted that in the measurement update, Eq. (23), the previously defined sigma points $x^i_{k|k-1}$ from Eq. (21) have been used for similarity with the EnKF algorithm and to save computational effort. However, the unscented transformation, based on the defined *a priori* state, $\hat{x}_{k|k-1}$, and covariance, $X_{k|k-1}$, estimate, can be used to create new sigma points for the measurement update. The use of these new sigma points can increase the performance of the estimator for nonlinear measurements, Simon [1].

Both the EnKF and UKF algorithms have been implemented in Python for further use with the model of the hydropower system.

4. Modelling

As mentioned above, a dynamic model of the waterway of a hydropower plant is used in this study. All modelling is done in OpenModelica, which is an open source Modelica-based modelling and simulation environment intended for industrial and academic usage.[6]

[5] Using Python package *numpy*, the Cholesky decomposition can be found by the *numpy.linalg.cholesky()* function.

[6] Some tutorials exist for Modelica — http://book.xogeny.com, and OpenModelica — https://goo.gl/76274H.

4.1. Hydropower library

For modelling the hydropower system, library *OpenHPL* is used. This is an in-house hydropower library, where different parts of the waterway components such as reservoir, conduit, surge tank, and turbine have been assembled. In this library, different waterway components of the hydropower system are described by both mass and momentum balances, and could include compressible/incompressible water or elastic/inelastic pipe walls. A more detailed overview of the mathematical models and methods used in this library is given in Vytvytskyi and Lie [11]; Splavska et al. [16].

4.2. Model presentation

In this study, a simplified system with incompressible water and inelastic pipe is considered. A block diagram that is relevant for this hydropower model is presented in Fig. 2. Here, the block diagram consists of drag and drop elements from *OpenHPL* that are structured in the same way as in the hydropower plant, compare with Fig. 1. These elements are also specified with appropriate geometry from Tables 1 and 2. Connectors that join each element hold information about the pressure in the connector and mass flow rate that flows through the connector — similar to the connection in the electrical circuit with voltage and current.

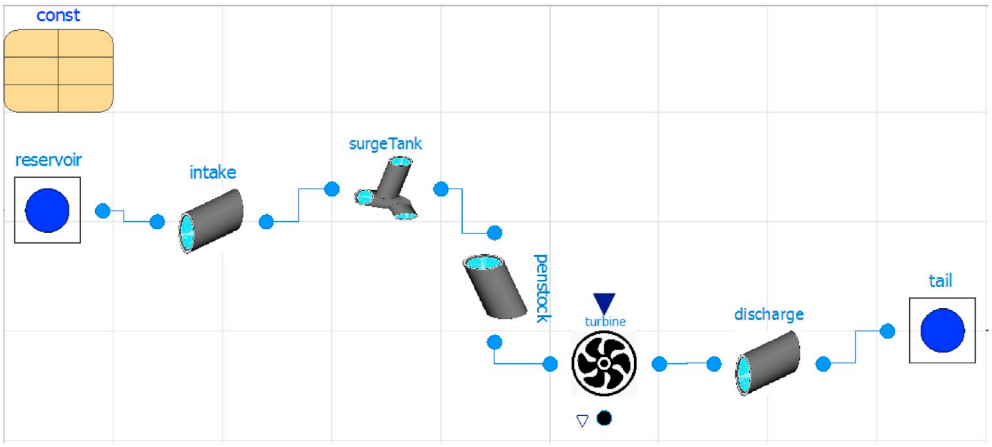

Fig. 2. Block diagram of the model of the hydropower system in OpenModelica. Modeled using *OpenHPL*.

For simplicity, the water levels in the reservoir and tail water are assumed to be constant. Regarding the model states, they consist of volumetric flow rates in the penstock, $\dot{V}_p$, and surge tank, $\dot{V}_s$, and the water height in the surge tank, h_s. The model has one input — turbine gate opening u_{tr}, and a few variables might be considered as measured outputs — turbine volumetric flow rate, $\dot{V}_{tr}$ (equals the flow rate in the penstock $\dot{V}_p$), pressure before the turbine (end of the penstock), p_{tr1}, and pressure in the manifold node (beginning of the penstock), p_n.

This hydropower model can be further used for assimilation with measured data. Using the Python API for OpenModelica, state estimation of this hydropower model is carried out in Python.

5. Results

5.1. Simulation overview

A number of cases for the measured output signal of the model are considered. In two cases, the output is described by only one measured variable. For a third case, two measured outputs are used in order to see if the combination of several measurement can improve the performance of the estimators. The following three cases are considered:

1. Measuring flow — using turbine volumetric flow rate, $\dot{V}_{tr}$, as the measured output, which means that one of the states is measured (turbine volumetric flow rate is the same as the flow rate in the penstock).
2. Measuring pressure — using either pressure before the turbine, p_{tr1}, or pressure in the manifold node, p_n.
3. Measuring both flow and pressure — using turbine volumetric flow rate, $\dot{V}_{tr}$, together with the inlet turbine pressure, p_{tr1}.

Measurement data from a real hydropower plant has not been available. Instead, synthetic/artificial measurements from hydropower model simulations are used. Hence, for all cases below, the hydropower model is first simulated separately to get appropriate synthetic measurements. Next, measurement noise, v_k, is added to the uncorrupted simulated measurement signal and then these synthetic measurements are used for the estimator simulations. Here, the measurement noise covariance is assumed from the accuracy of the measurements and depends on the nominal value of the measured variable. The mean of the measurement noise v_k is the same for all the cases, $\bar{v}_k = 0$, but the noise covariances V_k are different for each case and are as follows:

- Turbine volumetric flow rate, $\dot{V}_{tr}$, measurement — with nominal value approximately 20 m^3/s and accuracy 1%; the measurement noise covariance is $V_k = 0.004$, and $v_k \sim \mathcal{N}(0,0.004)$.
- Inlet turbine pressure, p_{tr1}, measurement — nominal value is approximately 50 bar and the accuracy is 1%; the measurement noise covariance is set to $V_k \approx 0.03$, and $v_k \sim \mathcal{N}(0,0.03)$.
- Manifold node pressure, p_n, measurement — nominal value is ca. 8 bar and the accuracy is 1%; the measurement noise covariance is set to $V_k \approx 0.0007$, and $v_k \sim \mathcal{N}(0,0.0007)$.

Additive random disturbance, w_k, is used in selected simulations to create the synthetic measurements. For simplicity, this random disturbance is given zero mean $\bar{w}_k = 0$ and covariance $W_k = 0.0001$ for all states, i.e. $w_k \sim \mathcal{N}(0,0.0001)$ — when used. When not used, $w_k \equiv 0$.

Assumed covariances are important design choices in the *estimator*. For optimal estimates, the covariances in the estimator should be equal to the covariances in the real, but unknown, random disturbances and noises. Here, synthetic measurements are used, and for that (unrealistic) case, the true covariances to use in the estimator are known. To test the robustness of the estimator, *disturbance* covariance in the estimator is set to either zero or $W_k = 10^{-4}$ — thus, the disturbance covariance used in the estimator may deviate from that used for drawing random disturbances for the synthetic measurements. Random measurement noise is always present, and perfect assumption of measurement covariance is used.

Table 3
The EnKF and UKF estimation results overview.

#	Available measurements from model	Fig.	Reality		Estimator		UKF results	EnKF result
			Random disturbance	Measurement noise	Random disturbance	Measurement noise		
1	Turbine flow rate	3	–	$V_k = 0.004$	–	$V_k = 0.004$	UKF a bit better for two states ($\dot{V}_s$, h_s). $\dot{V}_p$ good for both.	
2	Turbine flow rate.Steady state	4	–	$V_k = 0.004$	–	$V_k = 0.004$	UKF and EnKF converge to the correct steady state value. EnKF converges faster.	
3	Turbine flow rate	5,6	–	$V_k = 0.004$	$W_k = 10^{-4}$	$V_k = 0.004$	Become much poorer than #1. Plus more fluctuations.	Become a bit poorer than #1. Plus more fluctuations.
4	Turbine flow rate	7	$W_k = 10^{-4}$	$V_k = 0.004$	$W_k = 10^{-4}$	$V_k = 0.004$	EnKF better than UKF for two states ($\dot{V}_s$, h_s). $\dot{V}_p$ good for both.	
5	Inlet turbine pressure	8	–	$V_k = 0.03$	–	$V_k = 0.03$	UKF better for h_s and almost the same for $\dot{V}_s$. $\dot{V}_p$ good for both.	
6	Inlet turbine pressure	9,10	–	$V_k = 0.03$	$W_k = 10^{-4}$	$V_k = 0.03$	Become much poorer than #4. Plus more fluctuations.	Become a bit better than #4. But more fluctuations.
7	Inlet turbine pressure	11	$W_k = 10^{-4}$	$V_k = 0.03$	$W_k = 10^{-4}$	$V_k = 0.03$	EnKF better than UKF for two states ($\dot{V}_s$, h_s). $\dot{V}_p$ good for both.	
8	Manifold pressure	12	–	$V_k = 0.0007$	–	$V_k = 0.0007$	EnKF a bit better for h_s and the same for $\dot{V}_s$. $\dot{V}_p$ good for both.	
9	Manifold pressure	13,14	–	$V_k = 0.0007$	$W_k = 10^{-4}$	$V_k = 0.0007$	Become poorer than #7. Plus more fluctuations.	Become poorer than #7. Plus more fluctuations.
10	Manifold pressure	15	$W_k = 10^{-4}$	$V_k = 0.0007$	$W_k = 10^{-4}$	$V_k = 0.0007$	EnKF better than UKF for two states ($\dot{V}_s$, h_s). $\dot{V}_p$ good for both.	
11	Turbine flow rate and inlet pressure	16	–	$V_k = 0.004V_k = 0.03$	–	$V_k = 0.004V_k = 0.03$	UKF tiny better for two states ($\dot{V}_s$, h_s). $\dot{V}_p$ good for both	
12	Turbine flow rate and inlet pressure	17,18	–	$V_k = 0.004V_k = 0.03$	$W_k = 10^{-4}$	$V_k = 0.004V_k = 0.03$	Become poorer than #11. Plus more fluctuations	Become poorer than #11. Plus more fluctuations.
13	Turbine flow rate and inlet pressure	19	$W_k = 10^{-4}$	$V_k = 0.004V_k = 0.03$	$W_k = 10^{-4}$	$V_k = 0.004V_k = 0.03$	EnKF better but still not really close to model for two states ($\dot{V}_s$, h_s). $\dot{V}_p$ good for both.	
14	Turbine flow rate and inlet pressure. More detailed model	20	–	$V_k = 0.004V_k = 0.03$	–	$V_k = 0.004V_k = 0.03$	EnKF and UKF show good results. Estimates do not vary a lot from #11	

For all cases, the simulations start from steady state and last for 60 s with a sample time of 0.5 s. A disturbance occurs at time 20 s with a closing of the turbine valve: in real systems, the turbine valve is ramped up and down to avoid excessive water hammer effects; in this study, we have used a more informative step change. To limit the damaging effect of water hammer, we have used a 3% step change. The initial state covariance is the same for all states, $X_1 = 0.01$. Results of state estimation for all cases are shown below, and Table 3 in Section 6 gives a description of all of the simulations with a summary of the estimation results.

The number of *realizations/particles* for the EnKF is set to $n_p = 50$ for all EnKF simulations in this study. The number of UKF sigma points is known from the number of the model states and equals 6. The difference between the number of sigma points for the UKF and the number of *realizations/particles* for the EnKF leads to approximately ten times faster simulation time for the UKF.

5.2. Flow measurement

First, a comparison of estimates from the two KF algorithms (UKF and EnKF) and the model simulations is done for the hydropower system with correct knowledge of zero random disturbance, see Fig. 3.

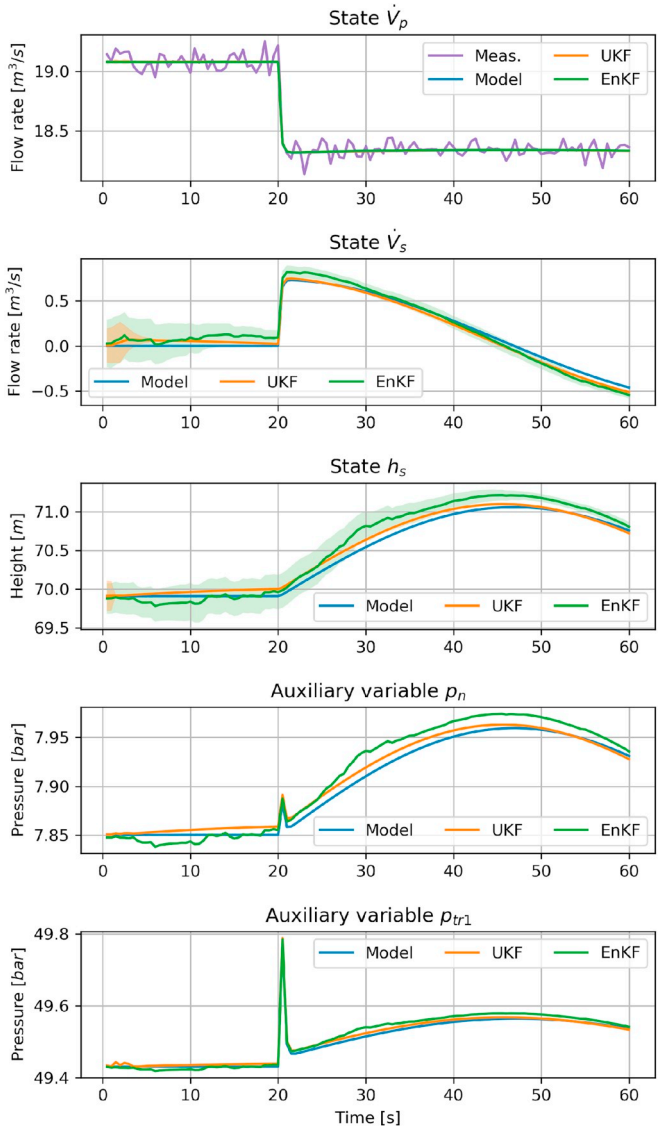

Fig. 3. State and auxiliary variable comparisons for the UKF and EnKF without random disturbance in the synthetic data, and with correct assumption of disturbance covariance in the estimators. Turbine flow rate is measured.

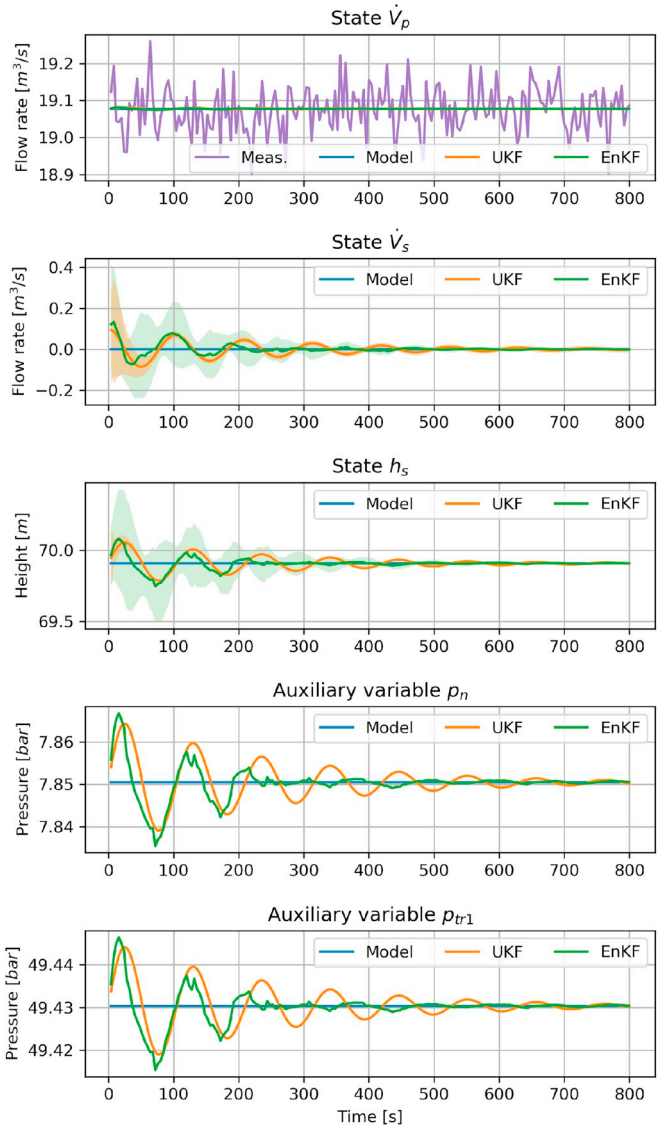

Fig. 4. Steady state simulation. State and auxiliary variable comparisons for the UKF and EnKF without random disturbance in the synthetic data, and with correct assumption of disturbance covariance in the estimators. Turbine flow rate is measured.

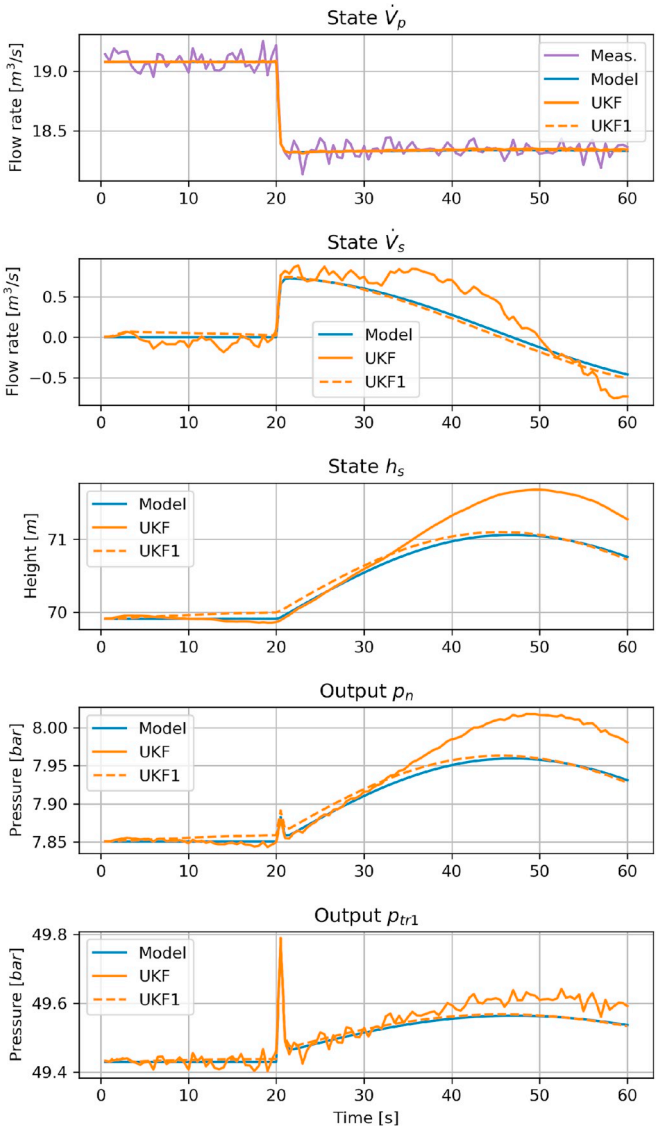

Fig. 5. State and auxiliary variable comparisons for the UKF with too large disturbance covariance and UKF1 with correct disturbance covariance. Turbine flow rate is measured.

Note that the information about the measurement noise is used in the estimators, for more details see Table 3. The results from the auxiliary variables (pressures p_{tr1} — before the turbine and p_n — in the manifold) are also shown in the figure for clarity. These auxiliary variables reflect the states because they are functions of the states. Furthermore, uncertainty ranges for the state estimates for both the UKF and EnKF are demonstrated by the filled area between two boundaries with the same but transparent color as for the related state estimates. These boundaries are calculated as two standard deviations of the state estimates, where the standard deviation is found as the square root of the diagonal element (variance) of the covariance matrix $X_{k|k}$.

Fig. 3 shows that the UKF provides better estimates than the EnKF for two states (surge tank flow rate $\dot{V}_s$, and water height h_s) that are not measured. It is also seen that the uncertainty range for the state estimates converges faster for the UKF than the EnKF, which might be a reason of the UKF's better performance.

To ensure that both the UKF and EnKF provide proper steady state results, a steady state simulation (with constant input signal u_{tr}) for an extended period of 800 s is performed for this case only, with the flow measurement, and without random disturbance, see Fig. 4. Here, the initial value for one of the estimator states deviates slightly from steady state in order to show that estimators results converge to the correct steady state values. From Fig. 4 it is seen that the EnKF needs a shorter time to converge to the steady state than the UKF.

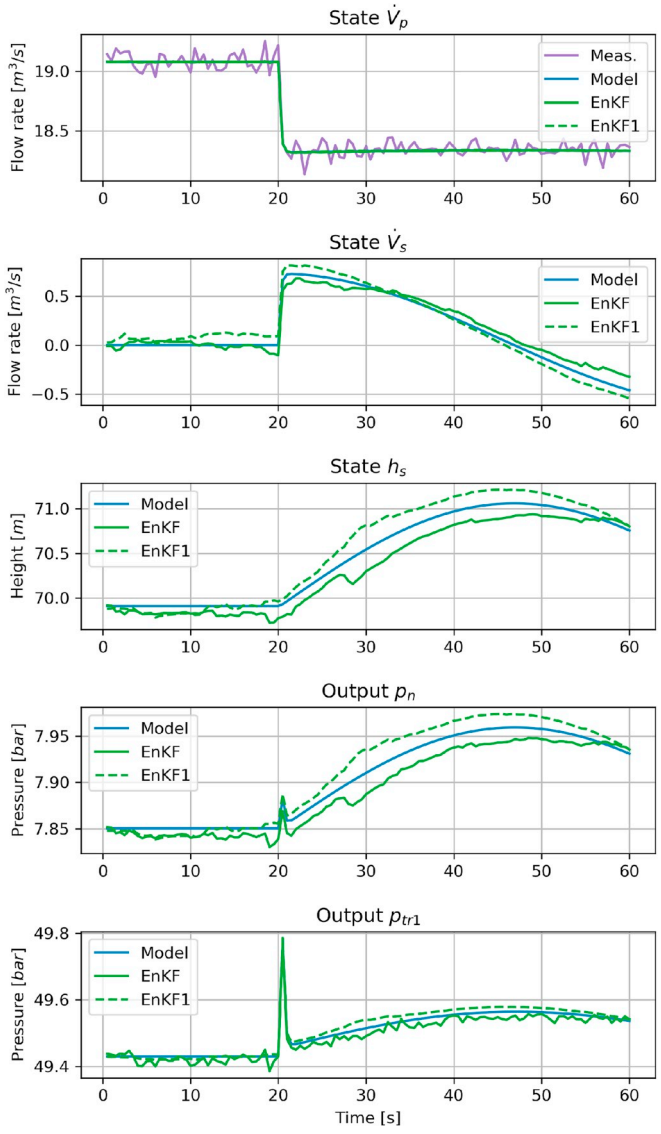

Fig. 6. State and auxiliary variable comparisons for the EnKF with too large disturbance covariance and EnKF1 with correct disturbance covariance. Turbine flow rate is measured.

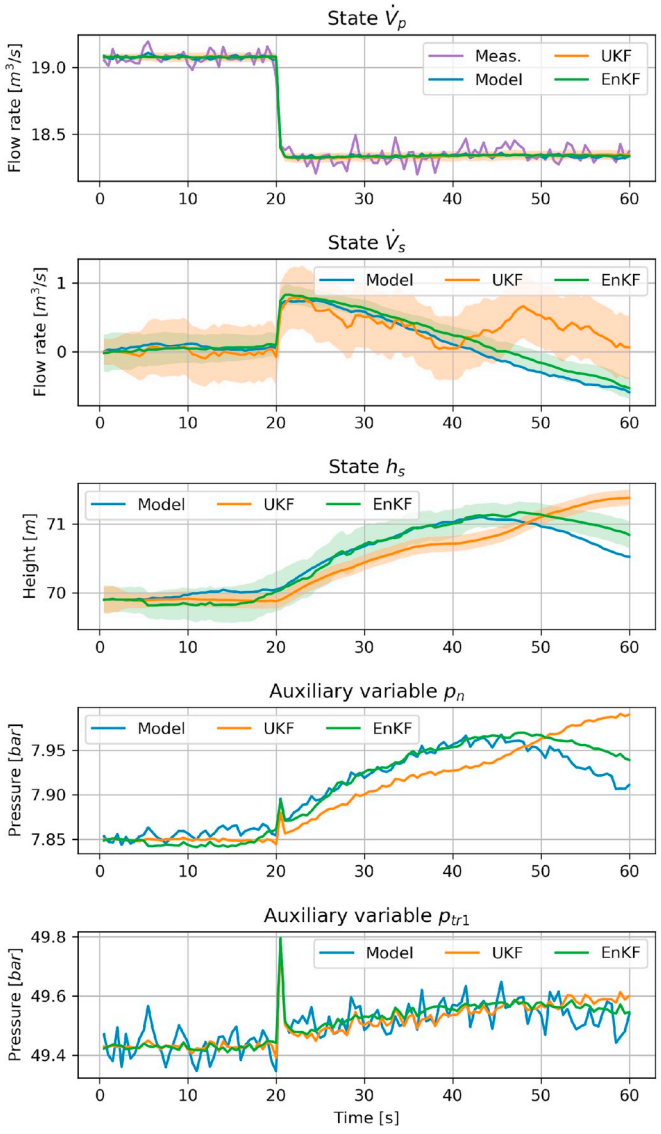

Fig. 7. State and auxiliary variable comparisons for the UKF and EnKF with measurement noise and random disturbance in the synthetic measurements, and correct assumption of disturbance covariance in the estimators. Turbine flow rate is measured.

In order to show the impact of the random disturbance on the UKF and EnKF, the estimators have been run with the same synthetic measurements, but with incorrectly assumed disturbance covariance $W_k \geq 0$ in the estimator, see Table 3. The comparison of the estimators with and without disturbance covariance is shown in Fig. 5 for the UKF and in Fig. 6 for the EnKF. In both figures, the estimators with disturbance covariance $W_k > 0$ are marked as "UKF" or "EnKF" and labels "UKF1" or "EnKF1" are used for the estimators with disturbance covariance $W_k \equiv 0$.

Both Figs. 5 and 6 show that assuming too large disturbance covariance in the UKF and EnKF makes the estimates more noisy; essentially, assuming larger disturbance covariance is equivalent to assuming lower measurement covariance, thus trusting the measurement too much, with more measurement noise "bleeding" through to the estimates. An interesting side result is that the estimation results of the UKF assuming incorrect disturbance covariance are much poorer than for the UKF with correct disturbance covariance.

Next, estimates of the UKF and EnKF are compared together with the model simulation for the hydropower system when the synthetic measurements include random disturbance w_k and correct disturbance covariance W_k is used in the estimators. For more details see Table 3. The results of this comparison are shown in Fig. 7. It is seen from the figure that the state estimates from the EnKF are close to the model

results, while the UKF estimates have more deviation in comparison to the model results.

5.3. Pressure measurement

In addition to the use of the flow rate measurement for the estimators, it is of interest to see how the UKF and EnKF behave when a pressure measurement is used. Both the inlet turbine p_{tr1} and the manifold node p_n pressures are of interest as measurements. The same set of dynamic simulations that have been done for the flow rate measurement case are performed for the case with pressure measurements. The use of the measured inlet turbine pressure for state estimation is first presented, and then the same state estimates are found based on the manifold node pressure measurement.

5.3.1. Measuring the inlet turbine pressure

Initially, the comparison of estimates from the UKF and the EnKF

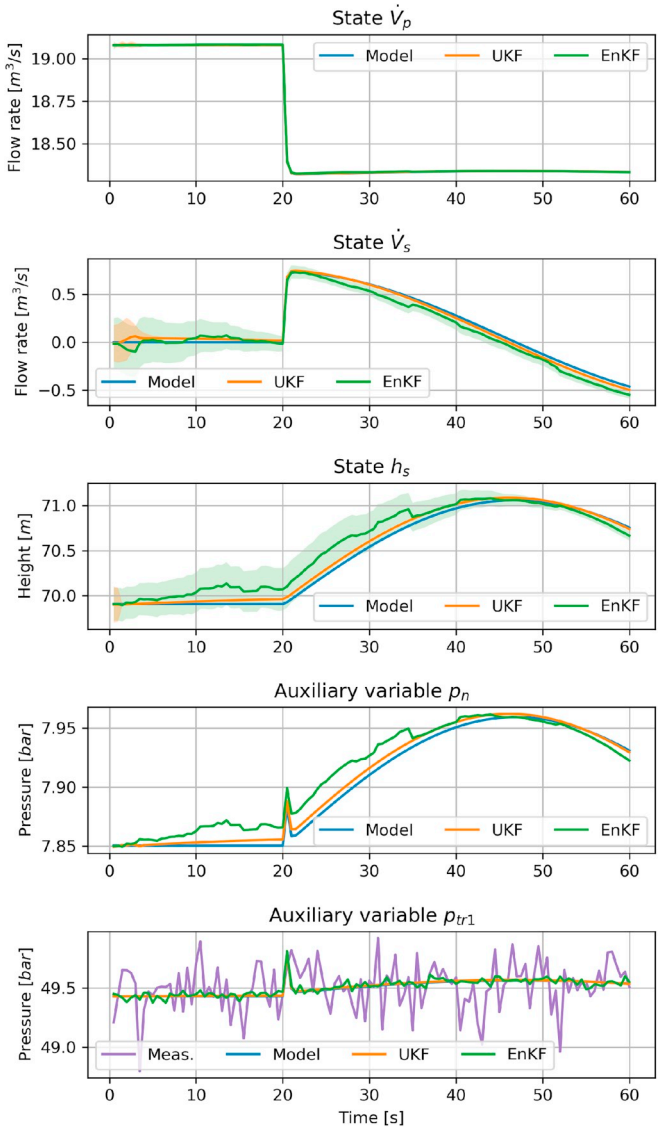

Fig. 8. State and auxiliary variable comparisons for the UKF and EnKF with measurement noise and without random disturbance + correctly assumed disturbance covariance in estimators. Inlet turbine pressure is measured.

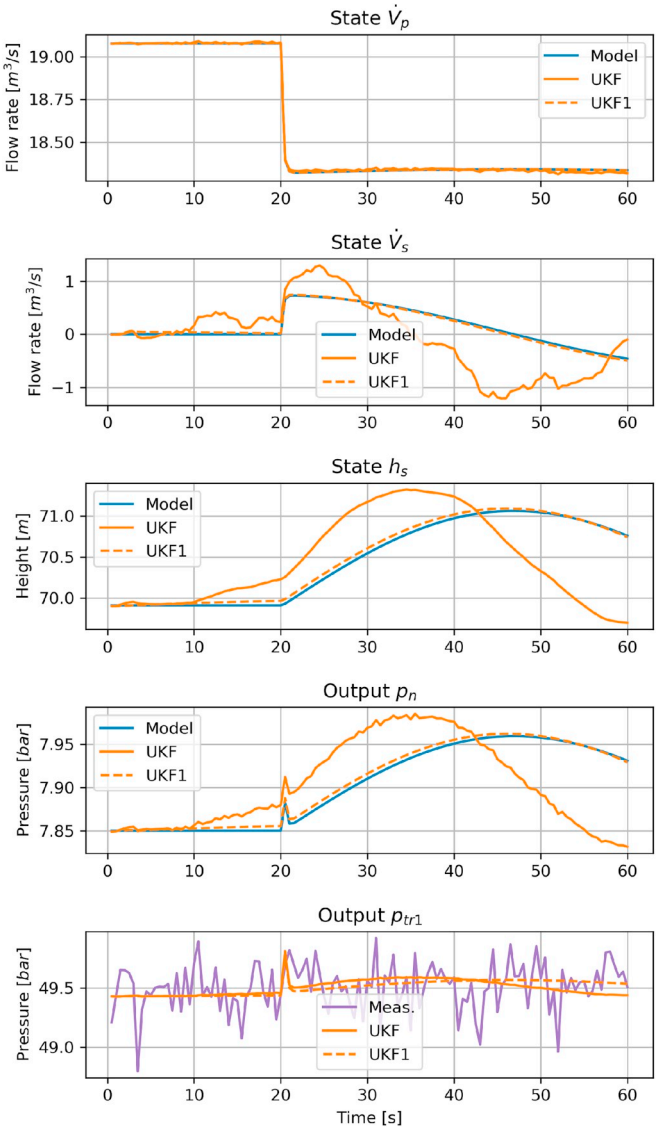

Fig. 9. State and auxiliary variable comparisons for the UKF with too large disturbance covariance and UKF1 with correct disturbance covariance. Inlet turbine pressure is measured.

are done for the hydropower system without random disturbance in the synthetic measurement and with correct assumption of disturbance covariance in the estimators, see Fig. 8. As when measuring the flow rate, information about the measurement noise is also added to the estimators, see Table 3.

Fig. 8 shows that the UKF provides a bit better estimates with lower variation with the model simulations than the EnKF for the states $\dot{V}_s$ and h_s. The estimates of the penstock flow rate look promising for both estimators.

Similarly, as for the case with measuring the flow rate, it is of interest to see the impact of incorrectly assumed disturbance covariance on the UKF and EnKF; the estimators have been run with the same pressure measurement as in the previous simulation, but with too large assumed disturbance covariance, see Table 3. The comparison of the estimators with too large assumed disturbance covariance (UKF/EnKF)

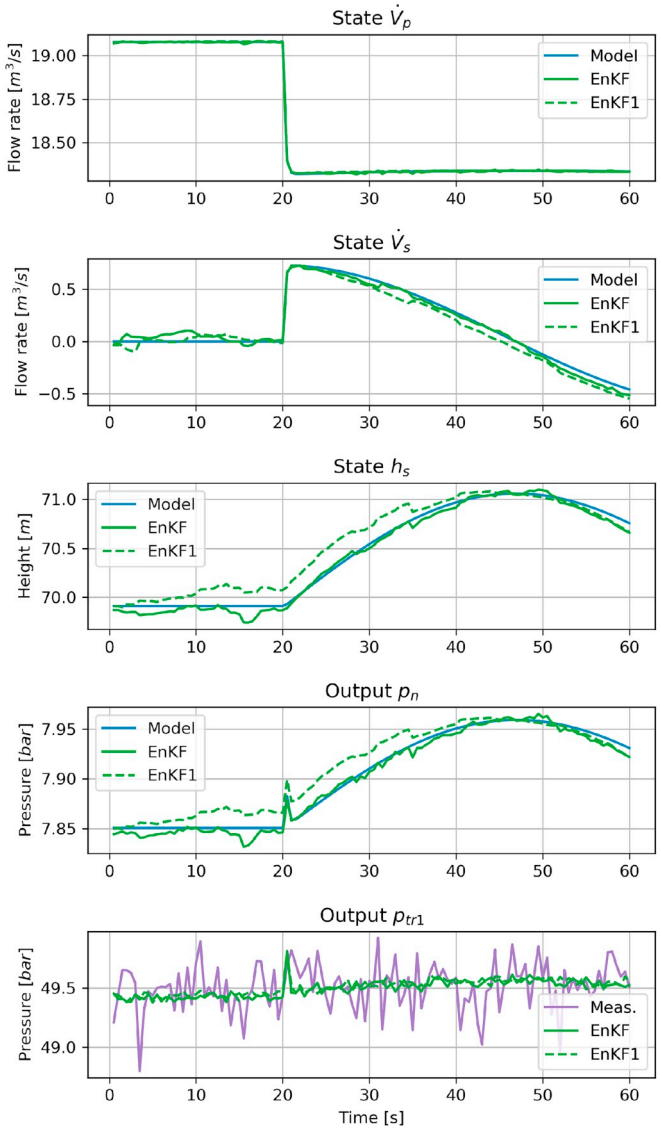

Fig. 10. State and auxiliary variable comparisons for the EnKF with too large disturbance covariance and EnKF1 with correct disturbance covariance. Inlet turbine pressure is measured.

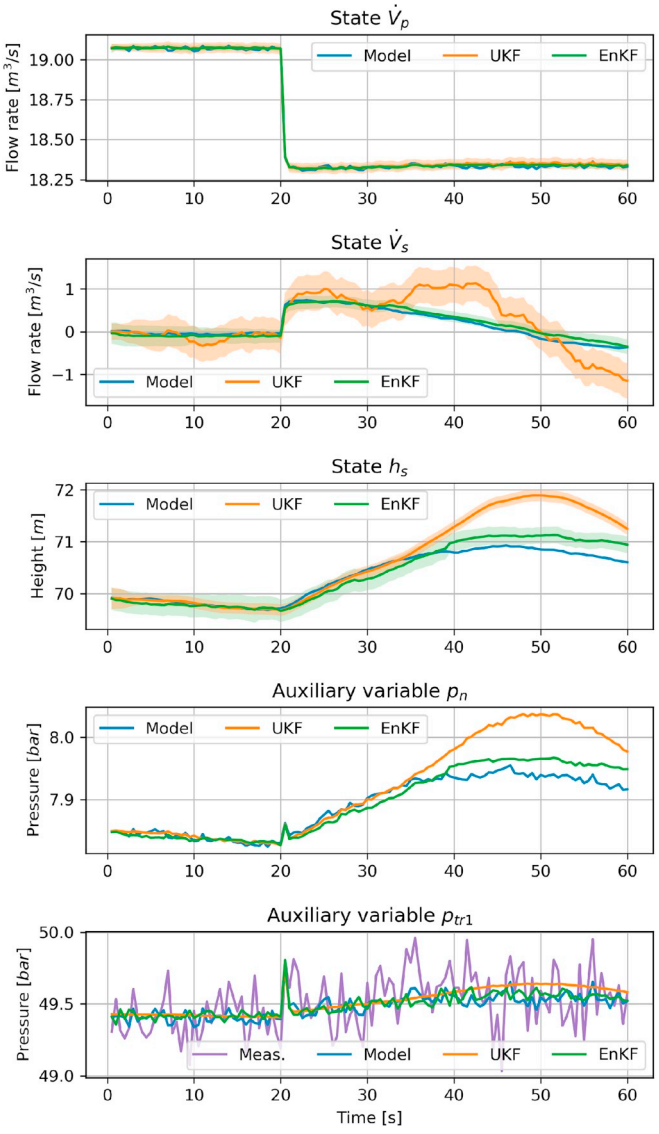

Fig. 11. State and auxiliary variable comparisons for the UKF and EnKF with correctly assumed covariances. Inlet turbine pressure is measured.

and with correct disturbance covariance (UKF1/EnKF1) are shown in Fig. 9 for the UKF and Fig. 10 for the EnKF.

From Figs. 9 and 10, it is seen that too large assumed disturbance covariance causes additional fluctuations in the estimates for both the UKF and the EnKF. However, this too large disturbance covariance assumption has less detrimental effect on the EnKF than on the UKF.

Next, the estimates with the UKF and EnKF with correctly assumed measurement noise and disturbance covariance are compared with the synthetic model simulation for the hydropower system. The results of this comparison are shown in Fig. 11. This figure shows that the EnKF

estimates deviate less from the model simulation than the UKF estimates. The estimates of the penstock flow rate is good for both estimators.

5.3.2. *Measuring the manifold pressure*

Next, the use of the manifold node pressure as the measurement is studied as an alternative to measuring the inlet turbine pressure. The comparison of estimates from two KF algorithms (UKF and EnKF) is done first for the hydropower system without random disturbance and with correct assumption of the disturbance covariance. The results are shown in Fig. 12; for more detailed simulation description see Table 3.

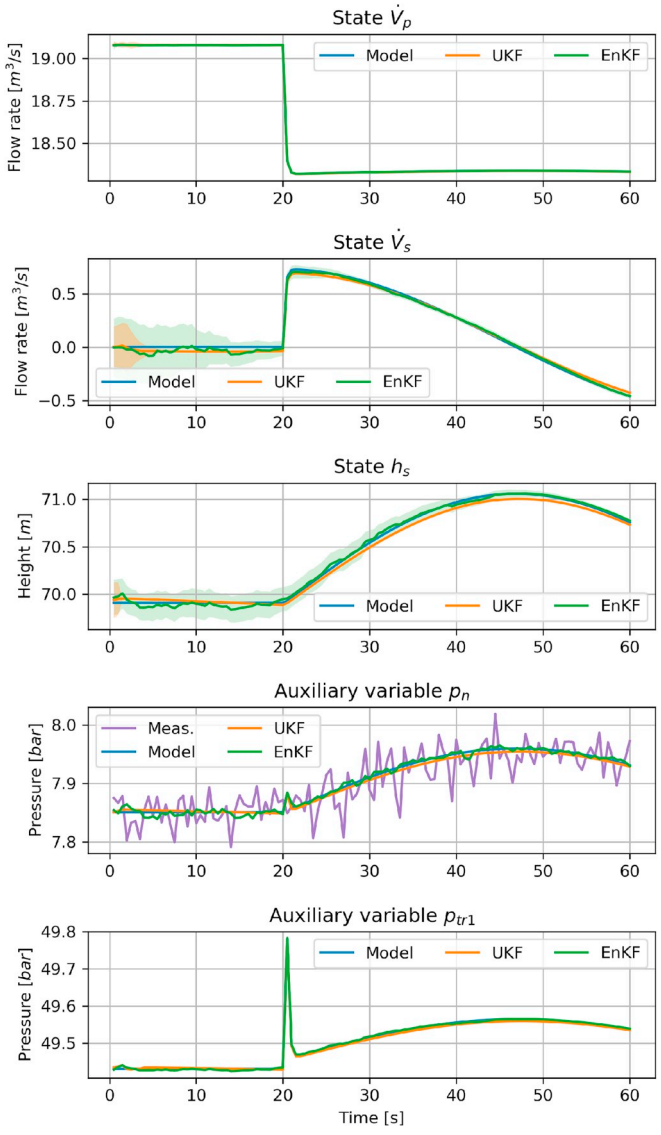

Fig. 12. State and auxiliary variable comparisons for the UKF and EnKF without random disturbance in the synthetic data, and with correct assumption of disturbance covariance in the estimators. Manifold pressure is measured.

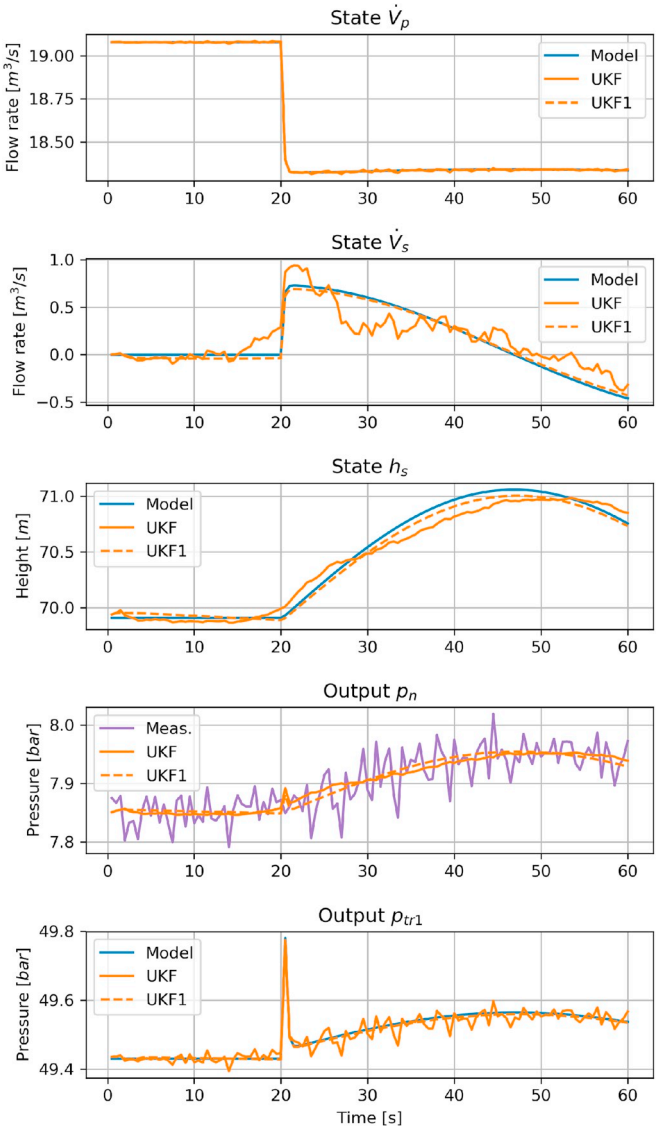

Fig. 13. State and auxiliary variable comparisons for the UKF with too large disturbance covariance and UKF1 with correct disturbance covariance. Manifold pressure is measured.

The UKF and EnKF estimates show low deviation from the model simulations. Some variation between the EnKF and UKF results is

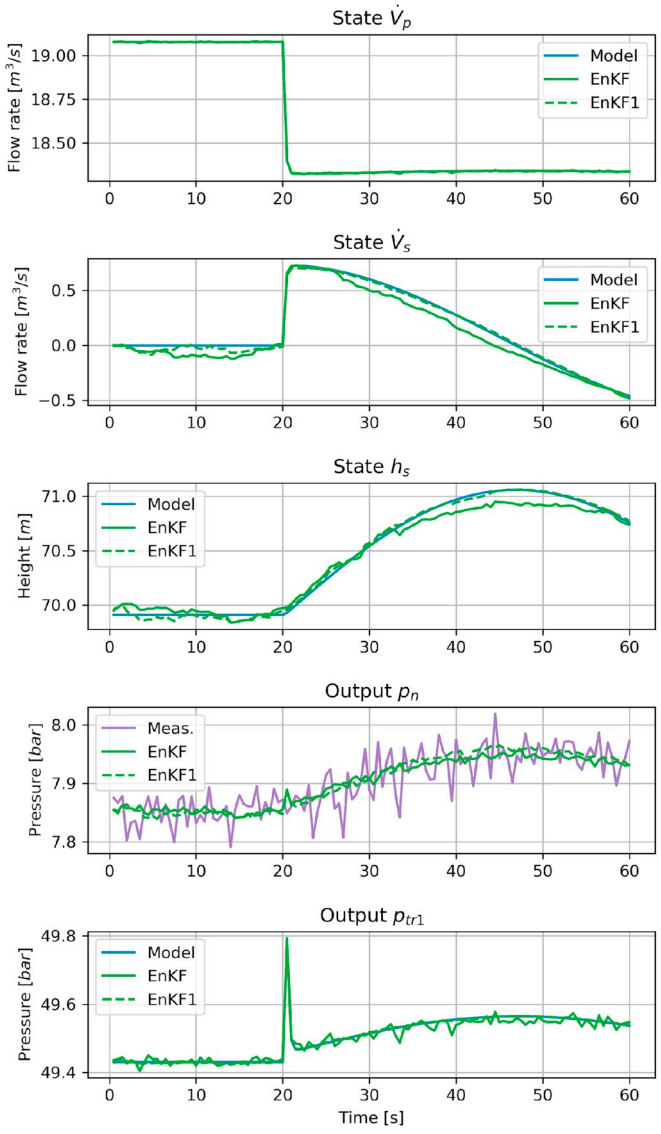

Fig. 14. State and auxiliary variable comparisons for the EnKF with too large disturbance covariance and EnKF1 with correct disturbance covariance. Manifold pressure is measured.

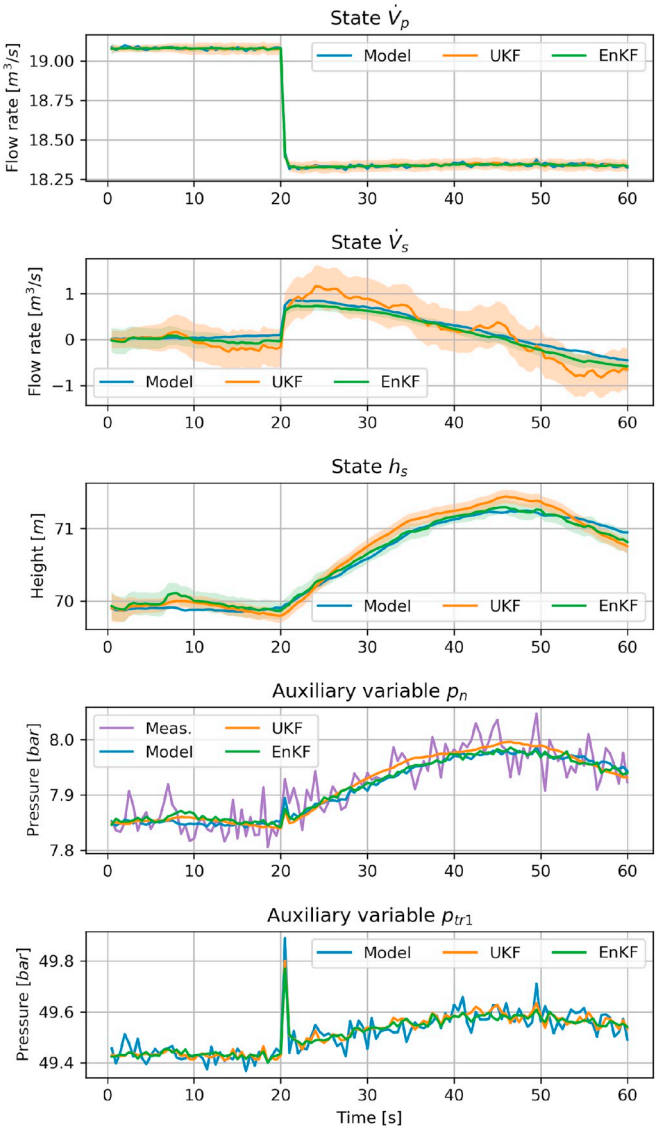

Fig. 15. State and auxiliary variable comparisons for the UKF and EnKF with measurement noise and random disturbance (both estimator and model). Manifold pressure is measured.

observed for the water height estimates of the surge tank, where the EnKF is closer to the model simulations. In the next comparisons, a too large covariance is assumed in the estimators, see Fig. 13 and Fig. 14. Similarly to the previous simulations, assuming too large disturbance covariance in the KFs leads to more deviation from the synthetic model simulation and more fluctuating estimates for both UKF and EnKF. In addition, the EnKF shows better results for the state estimates of the hydropower system with random disturbance, see Fig. 15. This is similar to the case with measuring the inlet turbine pressure.

5.4. Measuring both outputs

In addition to the presented cases with only one measured output, it is of interest to see if the use of two measurements can improve the

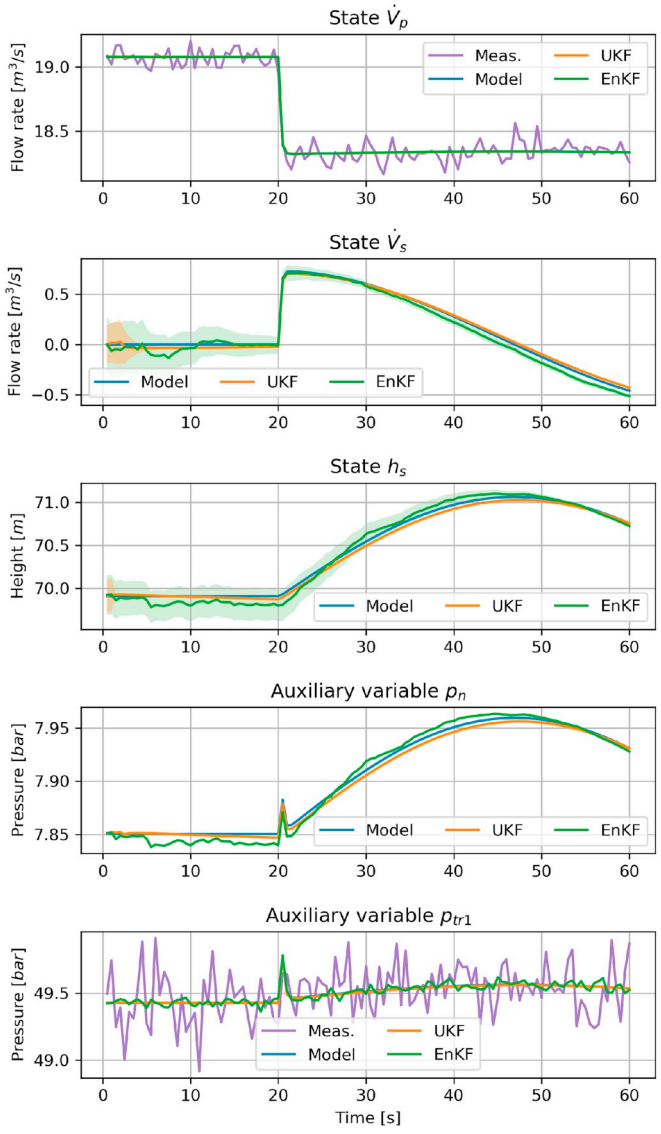

Fig. 16. State and auxiliary variable comparisons for the UKF and EnKF with measurement noise, without random disturbance, and with correctly assumed disturbance covariance in the estimators. Both pressure and flow rate are measured.

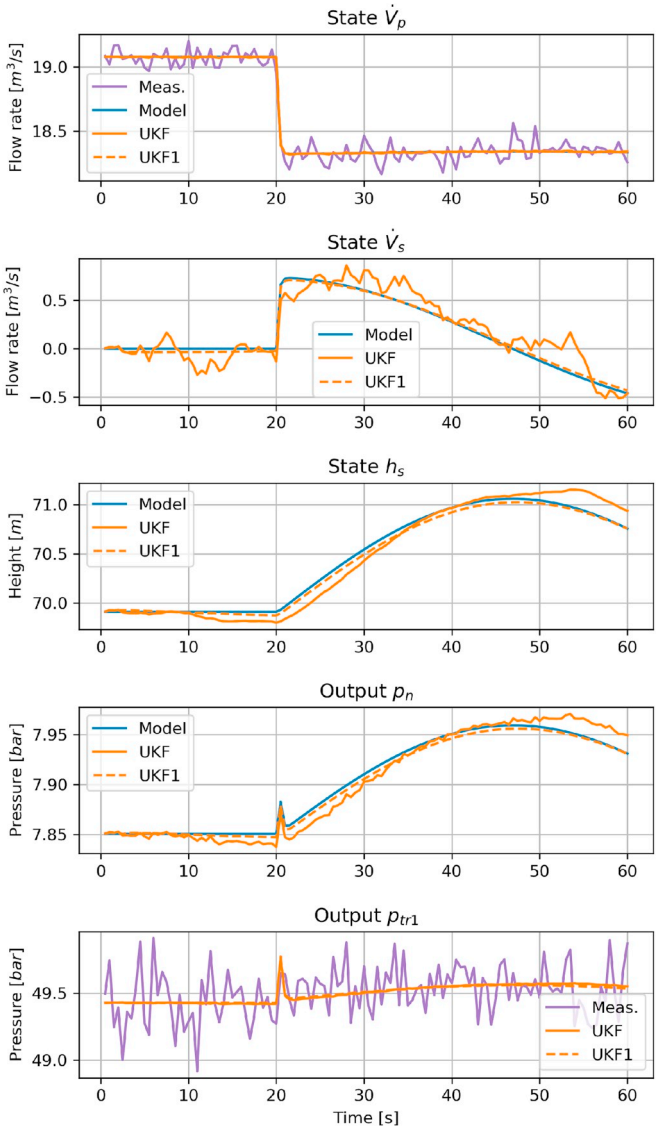

Fig. 17. State and auxiliary variable comparisons for the UKF with too large disturbance covariance and UKF1 with correct disturbance covariance. Both pressure and flow rate are measured.

performance of the estimators. Thus, both the turbine flow rate and the inlet turbine pressure are considered as measurements. The same set of dynamic simulations that have been done for previous cases are also performed for this case. A more detailed description of the simulations is found in Table 3. The results of this case with two measured outputs, hydropower model without random disturbance as well as correctly assumed covariance matrices in the estimators are given in Fig. 16.

It is seen from the figure that both the UKF and EnKF estimators provide good estimates and improve their results in comparison to the cases with only one measurement.

Then, in the same way as has been done in the previous cases, the impact of the assumed disturbance covariance on the UKF and EnKF is considered. The estimators have been run with the same two measurements, and with too large assumed disturbance covariance, see Table 3. The comparison of the estimators with too large assumed covariance (UKF, EnKF) and with correctly assumed disturbance (UKF1, EnKF1), respectively, are shown in Fig. 17 for the UKF and Fig. 18 for the EnKF.

Both figures show that the estimators reduce their performance when assuming too large disturbance covariance: the state estimates

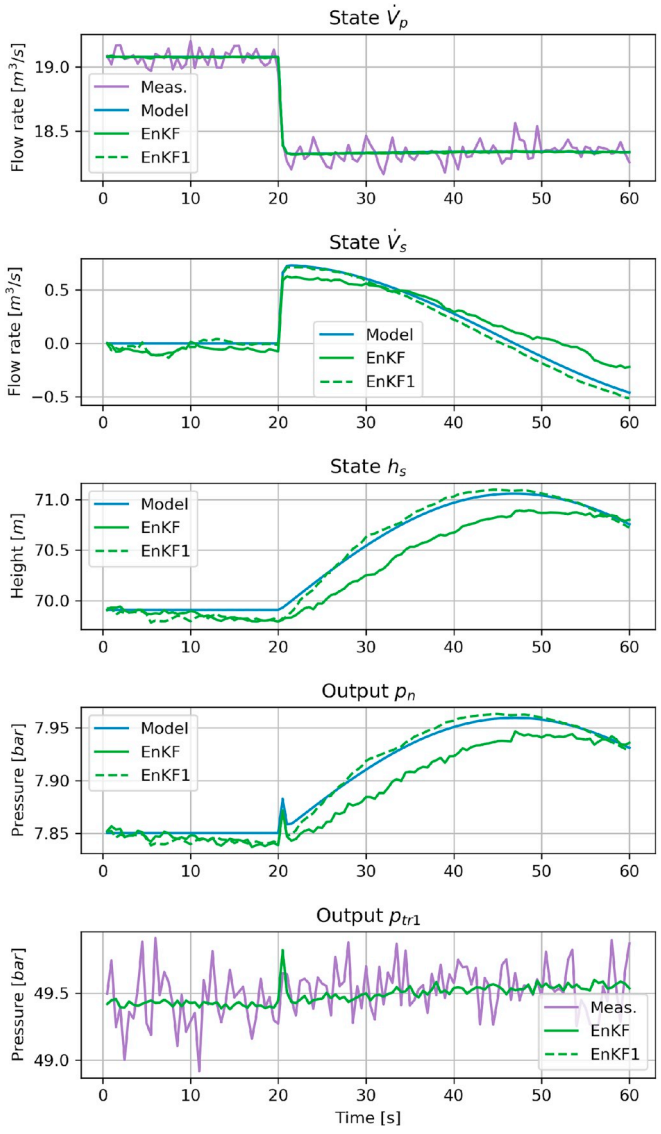

Fig. 18. State and auxiliary variable comparisons for the EnKF with too large disturbance covariance and EnKF1 with correct disturbance covariance. Both pressure and flow rate are measured.

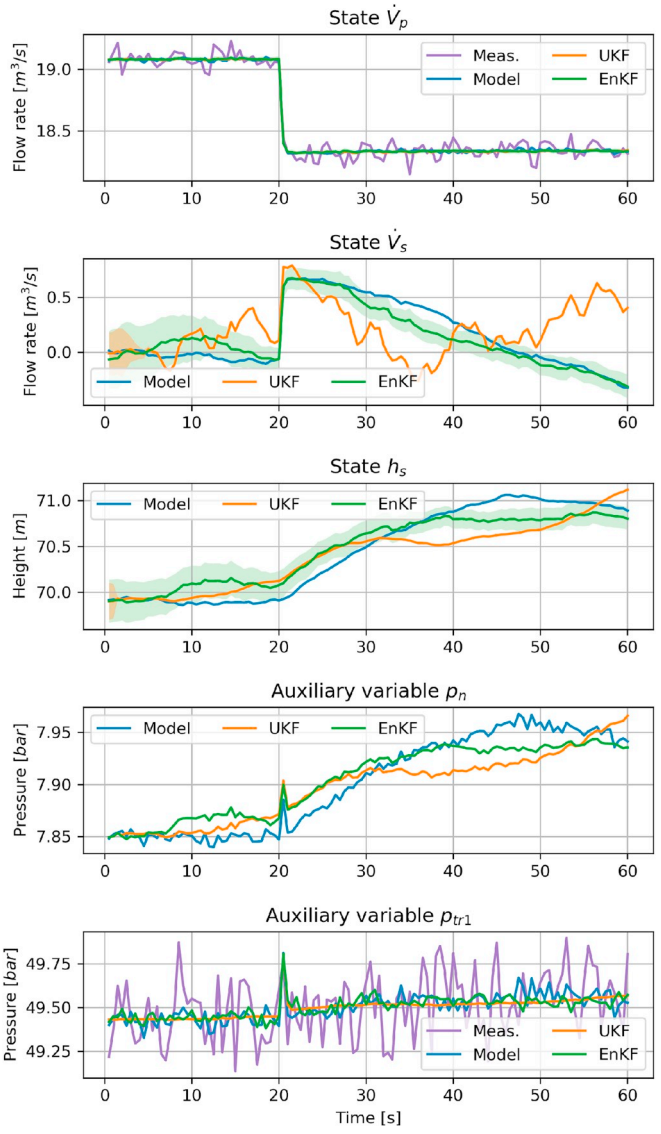

Fig. 19. State and auxiliary variable comparisons for the UKF and EnKF with measurement noise and random disturbance, and with correctly assumed disturbance covariance in the estimators. Both pressure and flow rate are measured.

become less accurate and noisier.

Finally, the estimates of the UKF and EnKF with correct assumptions of covariance matrices, and synthetic measurements/variables with random disturbance are compared. The results of this comparison are shown in Fig. 19. It is seen from this figure that the EnKF estimates deviate less from the model simulation than the UKF does.

5.5. *Measurements from a more detailed model*

It is of interest to see how the estimators behave when the synthetic measurements are based on a more detailed/realistic model while the simple model is used for the estimators. The detailed model used for the

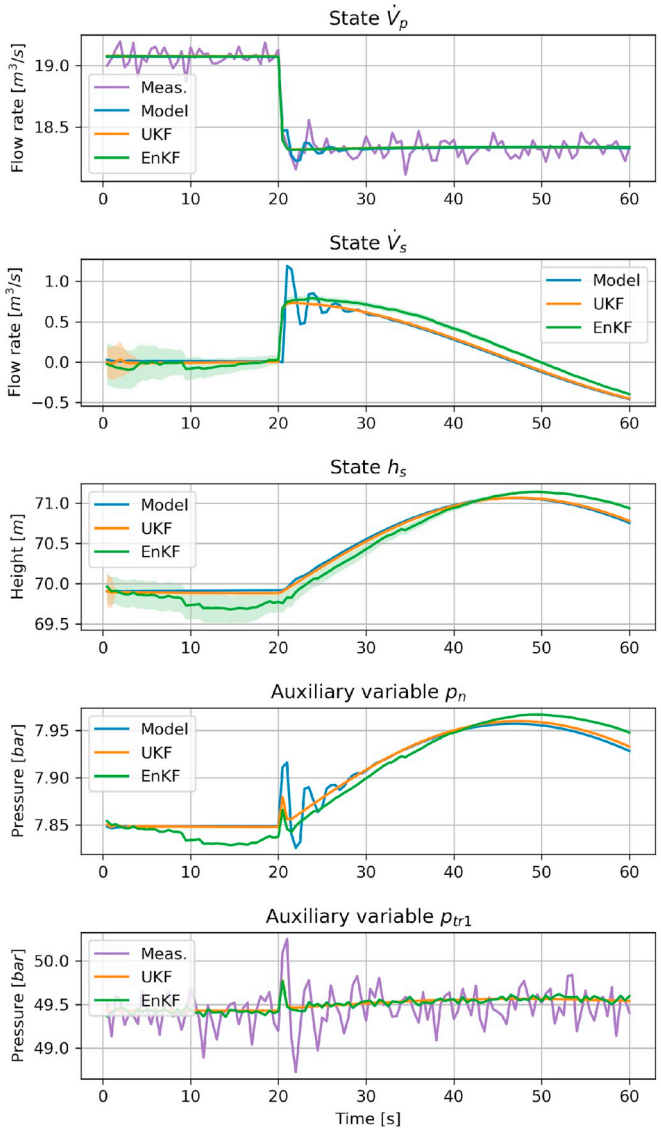

Fig. 20. State and auxiliary variable comparisons for the UKF and EnKF with measurement noise and without random disturbance in the detailed simulations/synthetic measurements. The estimators use correct information about covariance matrices. Both pressure and flow rate are measured.

synthetic measurements is similar to the model presented above, but includes water compressibility and pipe elasticity in the penstock, see Vytvytskyi and Lie [11] for more information about this model.

Similarly to the final case above, both the turbine flow rate and the inlet turbine pressure are considered as measurements. No random disturbance is used in detailed model simulation, and random measurement noise is added to create the synthetic measurements. The estimators use correct assumptions about the covariance matrices. The results of state estimation for this case are given in Fig. 20.

It is seen from the figure that the UKF provides a bit better estimates than the EnKF for two states. However, the estimators' results do not vary a lot from the case where the measurements have been provided from the simple hydropower model.

6. Discussion and conclusions

Based on the simulations, the observations of the EnKF and the UKF estimation results are structured in a table for better comparison and analysis, see Table 3.

Regarding the presented estimation results from both the UKF and EnKF, it is clearly observed that the UKF and EnKF estimates show good results for the penstock flow rate. Specifically, the results are promising for the cases where the flow rate is not measured. The estimates from the UKF and EnKF for two other states (the surge tank flow rate and water height) deviate more from the model simulations than the estimates for the penstock flow rate; the results for these other states are still useful, though.

In general, both the UKF and the EnKF appear to give good results when the estimators use correct information about covariance matrices — whether there is random disturbance or not. In real life, the "correct" information about covariance matrices is not known.

When the estimator assumes a larger disturbance covariance than the real system has, the estimates become noisy. This is to be expected: assuming too large disturbance covariance is akin to assuming too low measurement noise covariance, which will lead to too much trust in the measurements, hence a too large Kalman gain, and "bleeding" of measurement noise into the estimates. It is interesting to observe that the UKF appears to give poorer estimates than the EnKF for this case. A possible explanation for this is that since the EnKF uses more particles than the number of sigma points in the UKF, the EnKF tends to smooth out this noise in a superior way as to what the UKF does.

Both the UKF and the EnKF give good results with a single pressure measurement (inlet turbine pressure or manifold node pressure); the UKF works fine with either pressure measurement, while the EnKF works best with the manifold node pressure measurement.

A case with two measurements, the turbine flow rate and the inlet turbine pressure, has also been considered. Combining two measurements leads to good performance for both estimators, and an improvement over using a single measurement. However, two measurements at different locations may be more informative, and should be also considered for a future study.

In almost all cases, the state covariance (uncertainty) converges faster for the UKF than the EnKF.

Regarding the choice of estimator algorithm, it is hard to make a final decision. The UKF has an advantage wrt. computational speed, but both the UKF and the EnKF are straightforward to parallelize, and with modern multicore/multi threading processors, this advantage is perhaps not vital. The EnKF appears to handle incorrect assumption about covariances better; this is also an important feature.

To summarize, it has been shown in this paper that state estimation based on the assimilation of a mechanistic model and measured data, might be used to improve the information for hydropower plants. Moreover, the hydropower mathematical model can be modeled simply by dragging, dropping, and connecting appropriate unit elements of the hydropower system using a visual modelling tool, e.g., our in-house hydropower Modelica library — *OpenHPL* in OpenModelica. For an OpenHPL based model, the model can be operated on in Python, e.g., doing state estimation via the Python API for OpenModelica.

References

[1] D. Simon, Optimal State Estimation: Kalman, H∞, and Nonlinear Approaches, John Wiley & Sons, 2006.
[2] S. Julier, J. Uhlmann, A new extension of the kalman filter to nonlinear systems, Proc. Of AeroSense: the 11th Int. Symp. on Aerospace/Defense Sensing, Simulations and Controls, 1997, https://doi.org/10.1117/12.280797 3068 – 3068.
[3] G. Evensen, The ensemble Kalman filter for combined state and parameter estimation, IEEE Control Syst. 29 (2009) 83–104, https://doi.org/10.1109/MCS.2009.932223.
[4] W. Zhou, B. Glemmestad, Implementation of unscented Kalman filter for nonlinear state estimation in hydropower plant, IEEE International Conference on Power System Technology (POWERCON) , 1 – 5, 2012, https://doi.org/10.1109/PowerCon.2012.6401460.
[5] L. Zou, C. Zhan, J. Xia, T. Wang, C. Gippel, Implementation of evapotranspiration data assimilation with catchment scale distributed hydrological model via an ensemble Kalman Filter, J. Hydrol. 546 (2017) 685–702, https://doi.org/10.1016/j.jhydrol.2017.04.036.
[6] L. Shi, L. Zeng, D. Zhang, J. Yang, Multiscale-finite-element-based ensemble Kalman filter for large-scale groundwater flow, J. Hydrol. 468–469 (2012) 22–34, https://doi.org/10.1016/j.jhydrol.2012.08.003.

[7] K. Murphy, Machine Learning: A Probabilistic Perspective. Adaptive Computation and Machine Learning, MIT Press, 2012.
[8] J.A. Farrell, M.M. Polycarpou, Adaptive Approximation Based Control: Unifying Neural, Fuzzy and Traditional Adaptive Approximation Approaches (Adaptive and Learning Systems for Signal Processing, Communications and Control Series), Wiley-Interscience, New York, NY, USA, 2006.
[9] T. Stokelj, R. Golob, Application of neural networks for hydro power plant water inflow forecasting, Proceedings of the 5th Seminar on Neural Network Applications in Electrical Engineering. NEUREL 2000 (IEEE Cat. No.00EX287), 2000, pp. 189–193, , https://doi.org/10.1109/NEUREL.2000.902410.
[10] R. Sacchi, M.C. Ozturk, J.C. Principe, A.A.F.M. Carneiro, I.N. da Silva, Water inflow forecasting using the echo state network: a Brazilian case study, Proceedings of the International Joint Conference on Neural Networks, 2007, pp. 2403–2408, , https://doi.org/10.1109/IJCNN.2007.4371334.
[11] L. Vytvytskyi, B. Lie, Comparison of elastic vs. inelastic penstock model using OpenModelica, Proceedings of the 58th Conference on Simulation and Modelling (SIMS 58) Reykjavik, Iceland, September 25th–27th, 2017, Linköping University Electronic Press, Linköpings Universitet, 2017, pp. 20–28, , https://doi.org/10.3384/ecp1713820.
[12] L. Vytvytskyi, B. Lie, Mechanistic model for Francis turbines in OpenModelica, IFAC-PapersOnLine 51 (2018) 103–108, https://doi.org/10.1016/j.ifacol.2018.03.018.
[13] B. Lie, S. Bajracharya, A. Mengist, L. Buffoni, A. Kumar, M. Sjölund, A. Asghar, A. Pop, P. Fritzson, API for accessing OpenModelica models from Python, Proceedings of the EuroSim 2016, Oulu, Finland, 2016.
[14] B. Efron, The Jackknife, the Bootstrap, and Other Resampling Plans, SIAM, 1982.
[15] S.J. Julier, J.K. Uhlmann, Unscented filtering and nonlinear estimation, Proc. IEEE 92 (2004) 401–422, https://doi.org/10.1109/JPROC.2003.823141.
[16] V. Splavska, L. Vytvytskyi, B. Lie, Hydropower systems: comparison of mechanistic and table look-up turbine models, Proceedings of the 58th Conference on Simulation and Modelling (SIMS 58) Reykjavik, Iceland, September 25th–27th, 2017, Linköping University Electronic Press, Linköpings Universitet, 2017, pp. 368–373, , https://doi.org/10.3384/ecp17138368.